International Journal of Heat and Mass Transfer 53 (2010) 3855–3861

Contents lists available at ScienceDirect

International Journal of Heat and Mass Transfer

journal homepage: www.elsevier.com/locate/ijhmt

A numerical analysis of slab heating characteristics in a walking beam type reheating furnace

Sang Heon Han [a,*], Daejun Chang [a], Chang Young Kim [b]

[a] Division of Ocean System Engineering, Korea Advanced Institute of Science and Technology, 373-1 Guseong-dong, Yuseong-gu, Daejeon 305-701, Republic of Korea
[b] Energy Research Department, Research Institute of Industrial Science and Technology, 32 Hyoja-Dong, Nam-Gu, Pohang City, Gyeongbuk 790-330, Republic of Korea

ARTICLE INFO

Article history:
Received 14 August 2009
Received in revised form 8 April 2010
Accepted 8 April 2010
Available online 4 June 2010

Keywords:
Reheating furnace
Slab heating characteristics
Turbulent combustion

ABSTRACT

Numerical analysis of slab heating characteristics in a reheating furnace has been accomplished using FLUENT, a commercial software. The phenomena in the furnace are periodically transient because the slabs are transported toward a rolling mill with every time interval controlled. Unsteady calculation has been performed to obtain a periodically transient solution. A User-Defined Function (UDF) program has been developed to process the movement of slabs because FLUENT cannot handle the movement using its default functions. When the mean temperature of a slab emitted to the rolling mill does not change, calculation is considered to have converged and is stopped. This convergence criterion is appropriate for achieving an analytical solution. With the boundary and initial conditions given, over 55 new slabs are inserted to get a converged solution. Skid posts and beams are included in the calculation because they disturb radiation heat transfer from hot combustion gas to the slabs. This article examines what the slabs experience in the furnace before they are emitted to the rolling mill and whether a slab emitted to the rolling mill satisfies the required slab conditions, such as target temperature and skid severity.

1. Introduction

In a reheating furnace, slabs are heated up to the temperature over 1523 K and then transported to the rolling mill. The second largest energy is consumed to reheat slabs before the rolling process in a hot strip mill, while the largest energy is expended in melting ore. A great deal of attention is needed to reduce this huge amount of energy consumption, which leads to the enhanced operating performance of a reheating furnace. Its thermal efficiency is closely correlated with environmental issue, since a decrease in energy consumption or promotion of fuel efficiency directly reduce a generation of carbon dioxide – one of greenhouse gases. Reduction of other pollutants such as NO_x, particulates, and unburned hydrocarbon is also another concern of reheating furnace.

An analysis of thermal efficiency of a furnace requires a precise investigation of combustion and flow characteristics inside it. Since the feature of hot gas flow field has the deterministic role in heating slabs, some burners inside the furnace are positioned slightly slanted with respect to the horizontal direction to have more hot gas flow reach the slabs. Sometimes, block walls, so called dam, are installed in the furnace to control the main hot flow and make the main flow stay longer inside the furnace. But these are not all the factors to determine heating efficiency. There exist other factors such as type of fuel, location of slabs, thermal properties of slabs, and geometry of slab supporting systems. Skid posts and skid beams, which are necessary for supporting and transporting slabs, actually act like obstacles for hot gas flow and disturb the flow to reach slabs. In addition, they intercept radiation from hot gas towards slabs. It is well known that slabs are mostly heated by radiation [1,2] so that the heating efficiency is lowered if radiation from hot gas to slabs is blocked by existence of such structures.

There have been many efforts to simulate thermo-fluid mechanical phenomenon in a reheating furnace. Zhang et al. [3] attempted to predict the thermal performance of a regenerative reheating furnace by using the commercial software, FLUENT. The furnace was simplified as rectangular shape and a slab of infinite length was fed into the furnace with a constant velocity. Kim and Huh [4,5] carried out an analysis for turbulent reactive flow and radiative heat transfer on the actual shape of a walking beam type reheating furnace by using FLUENT. They calculated steady-state rates of heat transfer to slabs with the given temperatures of slabs. Hsieh et al. [6] calculated three-dimensional turbulent reactive flow with more complex geometry than Kim and Huh. They included skid beams and posts in the geometry. In the works of Refs. [3–7], all the authors used the given temperature data of slabs to compute steady flow and

* Corresponding author. Tel.: +82 42 350 1582; fax: +82 42 350 1510.
E-mail address: freezia@kaist.ac.kr (S.H. Han).

0017-9310/$ - see front matter © 2010 Elsevier Ltd. All rights reserved.
doi:10.1016/j.ijheatmasstransfer.2010.05.002

Nomenclature

$C_{p,k}$	specific heat of kth species, J/(kg K)
F	mixture fraction
f''	mixture fraction variance
k	turbulent kinetic energy, m^2/s^2
h	specific enthalpy, J/kg
I	radiation intensity, $W/(m^2$ sr)
I_b	blackbody radiation intensity, W/(m^2 sr)
$\vec{n}$	unit normal vector, m
q^R	radiative heat flux, W/m^2
$\vec{r}$	position vector, m
$\vec{s}$	unit direction vector, m
t	time, s
T	temperature, K
u_i	velocity components, m/s
Y_k	mass fraction of kth species

Greek symbols

ε	turbulent dissipation or emissivity
κ	absorption coefficient, m^{-1}
μ	molecular viscosity, kg/s m
μ_t	turbulent viscosity, kg/s m
ρ	density, kg/m^3
φ	representative variable
σ	Stefan–Boltzmann constant, $=5.67\times10^{-8}$ W/(m^2 K^4)
Ω	solid angle

Subscripts

i, j	coordinate direction or indexes
k	index for element or species
w	wall

temperature field. Huang et al. [7] predicted the temperature of a slab through steady state calculation. They modeled the slabs as a laminar flow having a very large viscosity.

No work predicting transient heating characteristics of slabs inside the furnace has been reported until now. Thermal efficiency of a reheating furnace and thermo-fluidic characteristics of the gas phase can be analyzed with the given temperature data of slabs, but the heating characteristic of slabs cannot be analyzed in this manner. Furthermore, improvement analysis of a reheating furnace cannot be made with a steady state approach. Unsteady calculation is required to analyze the heating characteristics of slabs inside the furnace and to improve furnace operating conditions and furnace geometry based on the analysis. In this study, unsteady calculation, including the movement of slabs, was performed to get a periodically transient solution using the commercial software FLUENT [8]. Because FLUENT cannot process slab movement with its default functions, a User-Defined Function (UDF) [9] program in C language was developed and linked to FLUENT. Skid posts and skid beams are included in the calculation to evaluate radiation shielding effects from hot gas to slabs. The heating characteristics of the slabs are numerically investigated and discussed in detail throughout this paper.

2. Mathematical formulation

2.1. Flow and energy equations

The unsteady, Favre-averaged continuity, momentum, energy, turbulent kinetic energy, eddy dissipation rate equations can be written as

$$\frac{\partial(\bar{\rho})}{\partial t}+\frac{\partial\bar{\rho}\tilde{u}_j}{\partial x_j}=0 \tag{1}$$

$$\frac{\partial(\bar{\rho}\tilde{u}_i)}{\partial t}+\frac{\partial\bar{\rho}\tilde{u}_j\tilde{u}_i}{\partial x_j}=\frac{\partial}{\partial x_j}\left[\mu\left(\frac{\partial\tilde{u}_i}{\partial x_j}+\frac{\partial\tilde{u}_j}{\partial x_i}\right)-\left(\frac{2}{3}\mu\frac{\partial\tilde{u}_k}{\partial x_k}\right)\right]-\frac{\partial\bar{p}}{\partial x_i}+\frac{\partial}{\partial x_j}\times(-\overline{\rho u_i'' u_j''}) \tag{2}$$

$$\frac{\partial(\bar{\rho}\tilde{h})}{\partial t}+\frac{\partial\bar{\rho}\tilde{u}_j\tilde{h}}{\partial x_j}=\frac{\partial}{\partial x_j}\left(\frac{\mu_t}{\sigma_h}\frac{\partial\tilde{h}}{\partial x_j}\right)+\widetilde{S}_h \tag{3}$$

$$\frac{\partial(\bar{\rho}\tilde{k})}{\partial t}+\frac{\partial\bar{\rho}\tilde{u}_j\tilde{k}}{\partial x_j}=\frac{\partial}{\partial x_j}\left[\left(\mu+\frac{\mu_t}{\sigma_k}\right)\frac{\partial\tilde{k}}{\partial x_j}\right]-\overline{\rho u_i'' u_j''}\frac{\partial\tilde{u}_j}{\partial x_i}-\bar{\rho}\tilde{\varepsilon} \tag{4}$$

$$\frac{\partial(\bar{\rho}\tilde{\varepsilon})}{\partial t}+\frac{\partial\bar{\rho}\tilde{u}_j\tilde{\varepsilon}}{\partial x_j}=\frac{\partial}{\partial x_j}\left[\left(\mu+\frac{\mu_t}{\sigma_\varepsilon}\right)\frac{\partial\tilde{\varepsilon}}{\partial x_j}\right]-C_{1\varepsilon}\frac{\tilde{\varepsilon}}{\tilde{k}}\left(\overline{\rho u_i'' u_j''}\frac{\partial\tilde{u}_j}{\partial x_i}\right)-C_{2\varepsilon}\bar{\rho}\frac{\tilde{\varepsilon}^2}{\tilde{k}} \tag{5}$$

where $\sim$ represents Favre-average and – represents time-average. The superscript $''$ denotes variance of Favre-average which can be used as in $\phi=\tilde{\phi}+\phi''$. $\widetilde{S}_h$ represents the source term containing heat generated by chemical reaction and divergence of radiative heat flux. The enthalpy is defined as

$$\tilde{h}=\sum_k \widetilde{Y}_k\int_{T_{ref}}^{T}C_{p,k}\,dT \tag{6}$$

The turbulent viscosity and the Reynolds stress and are assumed to be

$$\mu_t=\bar{\rho}C_\mu\frac{\tilde{k}^2}{\tilde{\varepsilon}} \tag{7}$$

$$\overline{\rho u_i'' u''}=\mu_t\left(\frac{\partial\tilde{u}_i}{\partial x_j}+\frac{\partial\tilde{u}_j}{\partial x_i}\right)-\frac{2}{3}\left(\mu_t\frac{\partial\tilde{u}_k}{\partial x_k}+\bar{\rho}\tilde{k}\right)\delta_{ij} \tag{8}$$

The values of model parameters used are $C_{1\varepsilon}=1.44$, $C_{2\varepsilon}=1.92$, $C_\mu=0.09$, $\sigma_h=0.9$, $\sigma_k=1.0$, and $\sigma_\varepsilon=1.3$.

2.2. Turbulent combustion model

The assumed PDF model is based on the assumptions of fast chemistry and unit Lewis number [10,11]. On these assumptions, the instantaneous thermo-chemical state of the fluid is related to a single conserved scalar quantity known as the mixture fraction, f, which is defined by

$$f=\frac{Z_k-Z_{k,ox}}{Z_{k,fuel}-Z_{k,ox}} \tag{9}$$

where Z_k is the elemental mass fraction for element, k. The subscript *ox* denotes the value at the oxidizer stream inlet and subscript *fuel* denotes the value at fuel stream inlet The conserved equation for the Favre-averaged mean and variance of f can be written as

$$\frac{\partial(\bar{\rho}\tilde{f})}{\partial t}+\frac{\partial\bar{\rho}\tilde{u}_j\tilde{f}}{\partial x_j}=\frac{\partial}{\partial x_j}\left(\frac{\mu_t}{\sigma_t}\frac{\partial\tilde{f}}{\partial x_j}\right) \tag{10}$$

$$\frac{\partial(\bar{\rho}\tilde{f}''^2)}{\partial t}+\frac{\partial\bar{\rho}\tilde{u}_j\tilde{f}''^2}{\partial x_j}=\frac{\partial}{\partial x_j}\left(\frac{\mu_t}{\sigma_t}\frac{\partial\tilde{f}''^2}{\partial x_j}\right)-C_g\mu_t\left(\frac{\partial\tilde{f}}{\partial x_i}\right)^2-C_d\bar{\rho}\frac{\tilde{k}}{\tilde{\varepsilon}}\tilde{f}''^2 \tag{11}$$

where the value for the constants σ_t, C_g, and C_d are 0.7, 2.86, and 2.0, respectively. Then, the instantaneous values of species mass fraction, density, and temperature in an adiabatic system can be computed as

$$\tilde{\phi} = \int_0^1 P(f)\phi(f)df \tag{12}$$

where $P(f)$ is assumed β-function which is characterized by $\tilde{f}$ and $\tilde{f}''^2$.

2.3. Radiative heat transfer

The radiant intensity at any position $\vec{r}$ along a path $\vec{s}$ through an absorbing, emitting, and non-scattering medium is given by [12]

$$\frac{dI(\vec{r},\vec{s})}{ds} = -\kappa I(\vec{r},\vec{s}) + \kappa I_b(\vec{r}) \tag{13}$$

where I is intensity, I_b is black-body intensity, and κ is an absorption coefficient. Black-body intensity depends only on the local temperature. The effect of radiation in energy equation is expressed in the form of divergence of radiative heat flux

$$-\nabla \cdot q^R = \kappa\left(4\pi I_b(\vec{r}) - \int_{4\pi} I(\vec{r},\vec{s})d\Omega\right) \tag{14}$$

2.4. Boundary and initial conditions

All the variables are specified in inlets. Neuman condition is used for specifying both outlet and symmetric boundaries. The furnace wall, the skid system wall, and the contact area between skid and slabs were assumed to be adiabatic. Initial condition is determined from the solution of steady state assumption that all the slabs have constant temperature of 293 K in the furnace.

The boundary condition for a diffusely emitting and reflecting wall can be denoted by

$$I(\vec{r}_w,\vec{s}) = \varepsilon_w I_b(\vec{r}_w) + \frac{1-\varepsilon_w}{\pi}\int_{\vec{s}'\cdot\vec{n}_w<0} I(\vec{r}_w,\vec{s}')|\vec{s}'\cdot\vec{n}_w|d\Omega' \tag{15}$$

where ε_w is the wall emissivity and $\vec{n}_w$ is the unit normal vector. The above equation illustrates that the leaving intensity at the wall is a summation of emitted and reflected intensities. Inlets and outlet for radiation boundary conditions are treated as if they are black-body wall. Since temperature is given and ε_i is 1.0 in inlet, intensity does not change with time. The wall intensity varies with time because incident radiation is periodically transient.

3. Results and discussion

3.1. Configuration of the furnace

Fig. 1 shows a half section of the reheating furnace. The furnace is symmetric with respect to the $z = 0$ plane, so calculations are performed on the half section of the furnace. The dimensions of the furnace are 34.8 m × 5.02 mv10.8 m and the furnace contains 29 slabs. The furnace is divided into three zones – preheating, heating, and soaking – which are depicted in Fig. 1. The preheating zone holds thirteen slabs; the heating zone holds nine slabs; and the soaking zone holds seven slabs. Slabs are mostly heated in the preheating and heating zones so most of the fuel is fed into furnace in these two zones.

A new slab is supplied from the left side wall of the furnace and transported step by step against the flow stream toward the exit. All slabs have the same dimensions and properties. The size of each slab is 1.02 m × 0.23 m × 9.6 m. Slabs are elevated 2.27 m from the furnace bottom and the distance between slabs is 0.16 m. There are 18 × 10 skid posts and 10 skid beams in the furnace to support the slabs inside the furnace. In this simulation, walking beams are assumed to remain at the same elevation as the static beams, but they are not in contact with the slabs, unlike the static beams. And walking and static beams are all simplified to have rectangular cross sections. A skid rail is put on each walking beam and it has a 5 mm × 5 mm cross section normal to the axial direction. The furnace is equipped with a total of 50 burners – 26 side burners in the lower zone and 24 axial burners in the upper zone. Each burner is simplified with two concentric circles. The inner circle is used for fuel passage and the annulus formed by two concentric circles is used for air passage. Flue gas is emitted from the furnace through an exhaust duct which is shown as outlet in Fig. 1.

The fuel is a mixture of COG (coke oven gas) and BOG (blast oven gas). The precise composition of the fuel is shown in Table 1. Heat of combustion of the fuel mixture is 14,433 KJ/m^3 at 273 K and 1 atm. The volumetric inlet flow rates of fuel and air are given in Table 2. Intake fuel temperature is 300 K and air temperature is 693 K. The equivalence ratio is 0.909 which is overall fuel lean with 10% of excess air. A relatively small amount of fuel is fed into the furnace in the soaking zone. The role of soaking zone is to make the inner temperature distribution inside the slab more uniform so temperature increase in the soaking zone is negligible. The swirl strength of inlet flow is set to be 0.3 for all the burners.

3.2. Simulation of the furnace

Thermo-fluid phenomena of the reheating furnace are periodically transient during the time interval of slab insertion. Unsteady calculation is performed to obtain a periodically transient solution. The calculation is done by feeding a slab into the furnace every time interval of slab insertion. When the mean temperature of slabs emitted to the rolling mill does not change, it is concluded that the calculation has converged. In this article, periodically changing phenomena during time interval of slab insertion is not discussed in depth, but heating characteristics of a slab during the residence time in the furnace are described precisely.

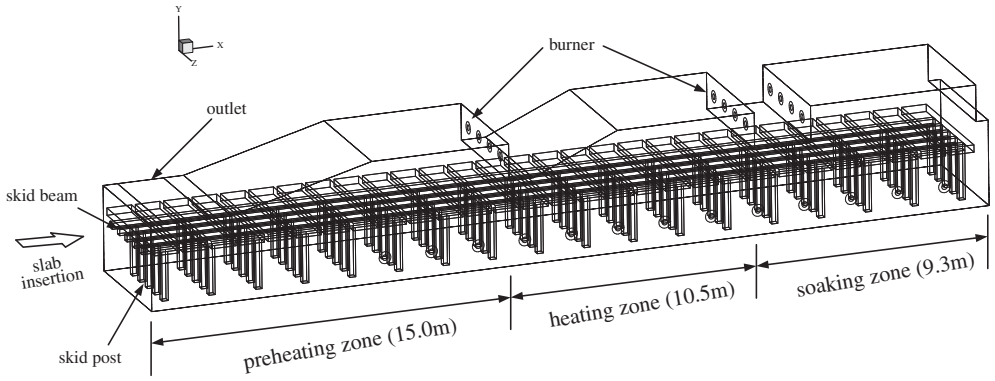

Fig. 1. Configuration of the furnace.

Fig. 2 shows the computational grid which is composed of 561,792 cells. The emissivity of walls is set to 0.75. The density of slabs is 7854 kg/m^3 and other properties of slabs are listed in Table 3. The insertion time interval of a slab is 256 s and the residence time of a slab in the furnace is 7474 s. The time step size for calculation was 16 s. The movement of slabs is processed by transporting temperature data from the previous location to the next location using a UDF program in C language. It is assumed that no time is spent for moving slabs.

The discrete ordinates (DO) model for radiation was used for the prediction of radiation [13,14]. The DO model is a flux type of method. A geometrical space is discretized into a finite number of control volumes and angular direction is also discretized into a finite number of control angles ($=N_\theta \times N_\varphi$). In this study, N_θ is equal to 4 and N_φ is equal to 8 with 32 discretized angular components of the radiation intensity. The inflow and outflow of radiant energy across the control volume faces are balanced with attenuation and augmentation of radiant energy within each control volume and each control angle. The absorption coefficient κ for gas medium is obtained by the weighted-sum-of-gray-gases model [15–17] which takes into account only participating molecules such as CO, CO_2, and H_2O.

Table 1
Composition of fuel mixture.

Species	Volume fraction (%)
H_2	0.564
CH_4	0.266
C_2H_6	0.029
CO	0.084
CO_2	0.031
O_2	0.003
N_2	0.023

Table 2
Burner inlet conditions (km^3/h).

	Preheating zone	Heating zone	Soaking zone	Total
Upper zone	4.28 (22.6%)	3.61 (19.0%)	1.39 (7.3%)	9.28 (48.9%)
Lower zone	4.36 (23.0%)	3.74 (19.8%)	1.57 (8.3%)	9.67 (51.1%)
Total	8.64 (45.6%)	7.35 (38.8%)	2.96 (15.6%)	18.95 (100%)

Table 3
Properties of slab.

Temperature (K)	Conductivity (W/m)	Specific heat (J/kg K)	Emissivity
$T < 473$	60.57	504.0	0.5
$473 < T < 673$	51.17	577.9	0.5
$673 < T < 873$	41.74	712.3	0.5
$873 < T < 1073$	34.04	892.1	0.5
$1073 < T < 1273$	28.08	730.8	0.6
$1273 < T$	29.81	672.0	0.6

Fig. 3(a) shows the time history of the mean temperature of slabs just before they move. When the calculation converges, the curve of mean temperature does not change and remains at a converged curve. This converging history is well depicted in the graph. As the time goes, curves stick to the converged one. The newer a slab is, the faster the mean temperature of the slab joins the converged curve. The mean temperature of the last slab joins the converged curve latest. Fig. 3(b) shows the mean temperature difference between the current slab and the previous slab just before slabs move. This graph is more intuitive than time history of mean temperature of slabs. As the time goes, curves converge to zero line. It took about 140 h to complete a calculation with a 3.12 GHz Pentium 5 PC.

Fig. 4 shows temperature contours on two planes. The plane of $z = 0.8$ m is the cross section through the center line of a top burner and the $y = 1.004$ m plane is the cross section through the side burners. Large, long flames are formed around the burners in the preheating and heating zones and very small scale flames are formed in the soaking zone. This is because less fuel is fed into the soaking zone. Another reason that only small flames are formed in the soaking zone is because gas flowing out of the top burners changes directions to the opposite side. Fig. 4(a) shows that the temperature of slabs is mostly raised in the preheating and heating zones. Slabs in the soaking zone experience little temperature elevation, which is reflected in Fig. 4(a).

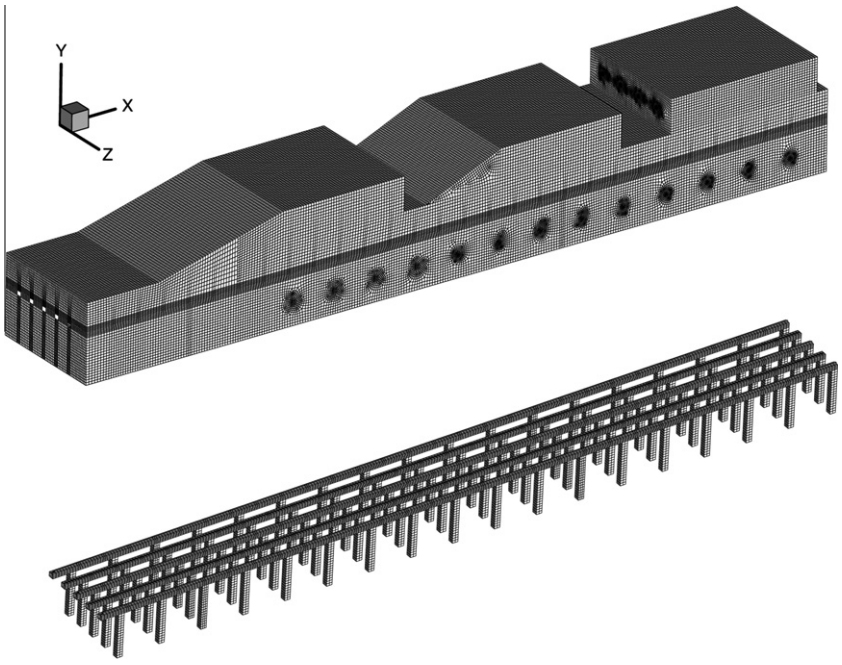

Fig. 2. Computational grid.

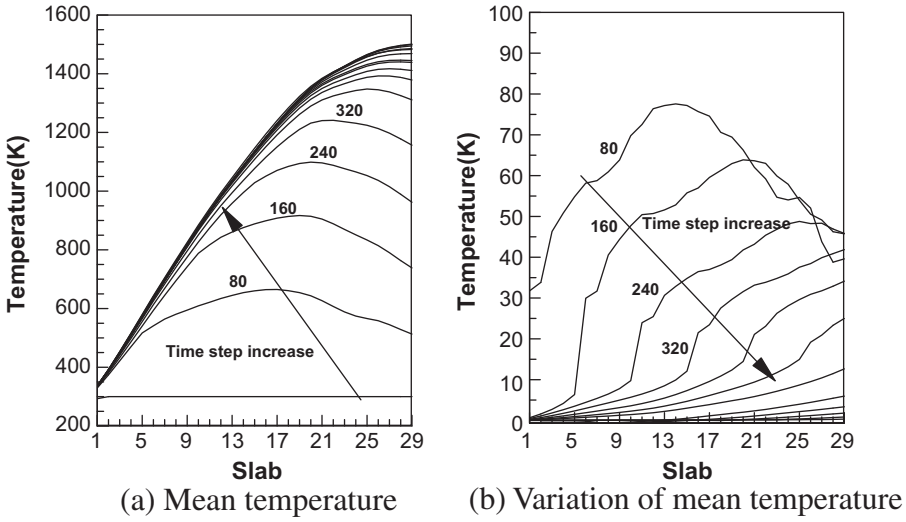

Fig. 3. Converging history.

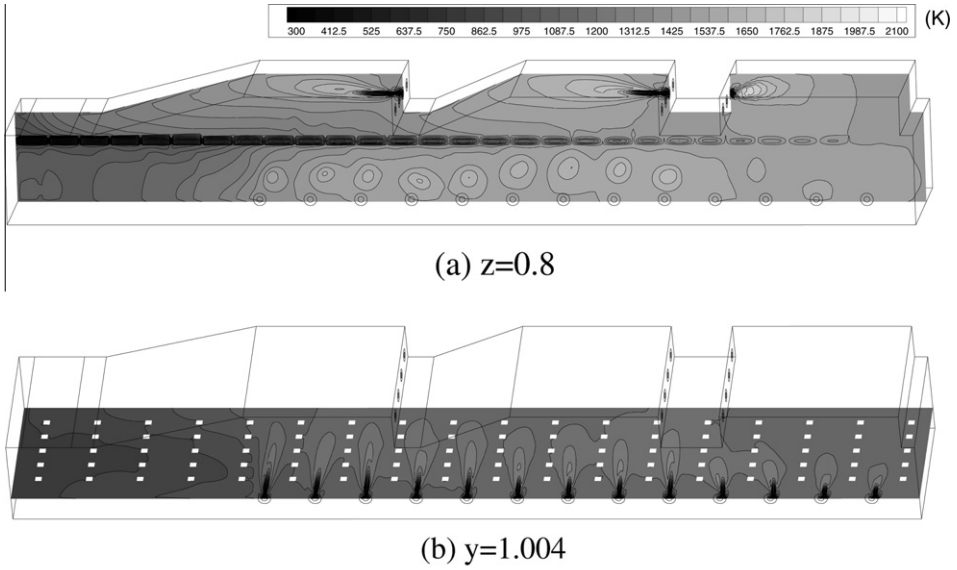

Fig. 4. Temperature contour just before move.

3.3. Heating characteristics of slabs

In the early stage of heating, isothermal contour lines are clustered around corners and edges which have larger thermal resistivity than the plane surface region. Isothermal lines, called skid marks, are also clustered around the contact areas between the slabs and the skid beams. Figs. 5 and 6 depict these phenomena. The history of skid marks on the lower surface of a slab can be clearly seen in Fig. 5. Temperature gradients in slabs are mostly due to the skid system. Although isothermal contour lines around corners and edges disappear before a slab arrives in the soaking zone, isothermal contour lines around contact areas still remain on the slab in the soaking zone. Skid marks are formed by skid system's shielding heat flux from hot combustion gas. While skid marks appear very clearly in the early stages, they disappear in the later stage-soaking zone.

The time-averaged total heat transfer rate to the slabs is 33,920 kW which corresponds to 46.1% of the total input energy. The total input energy is composed of the fuel energy which is 61,680 kW and the sensible energy of the air which is 11,880 kW. To investigate the heating characteristics in view of heat flux, various heat fluxes to the slabs are depicted in Fig. 7. The slabs in the preheating and heating zones receive a large portion of heat flux generated from the combustion gas. On the other hand, heat flux becomes weak in the soaking zone because the slabs in the soaking zone have already experienced enough heating in previous zones that the temperature difference between the hot gas and slabs remains very small. Slabs are mainly heated by radiation. Convective heat flux contributes little to heating slabs. The percentage of radiative heat flux was 86% at minimum at the first slab, it rose to 95% at the 8th slab, it went up to 99% in the soaking zone, and it has the average value of 96%.

Radiative heat flux to the upper or the lower surface of a slab continues to grow from the insertion of the slab until the flux reaches its maximum. Newer slabs meet more used flue gas and receive less radiative heat flux. Since hot gas flows from the side burners turn

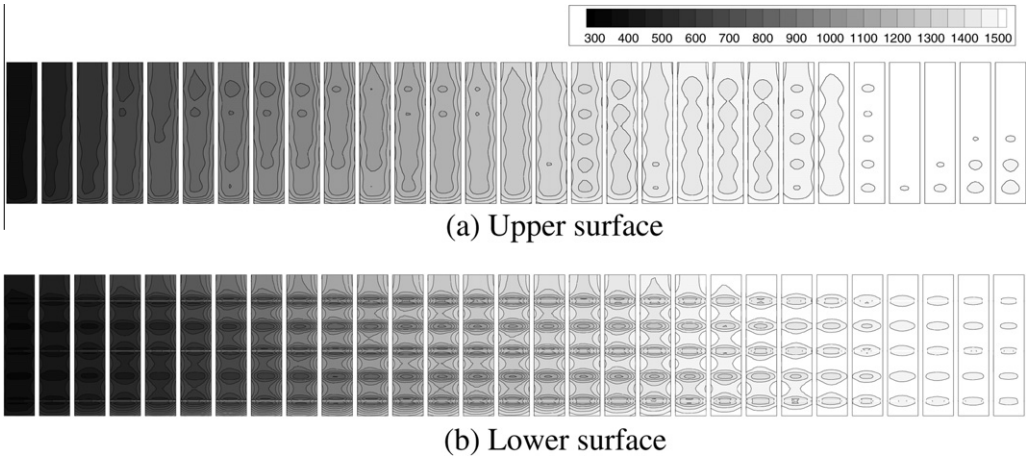

Fig. 5. Temperature contour of slabs in the furnace just before move.

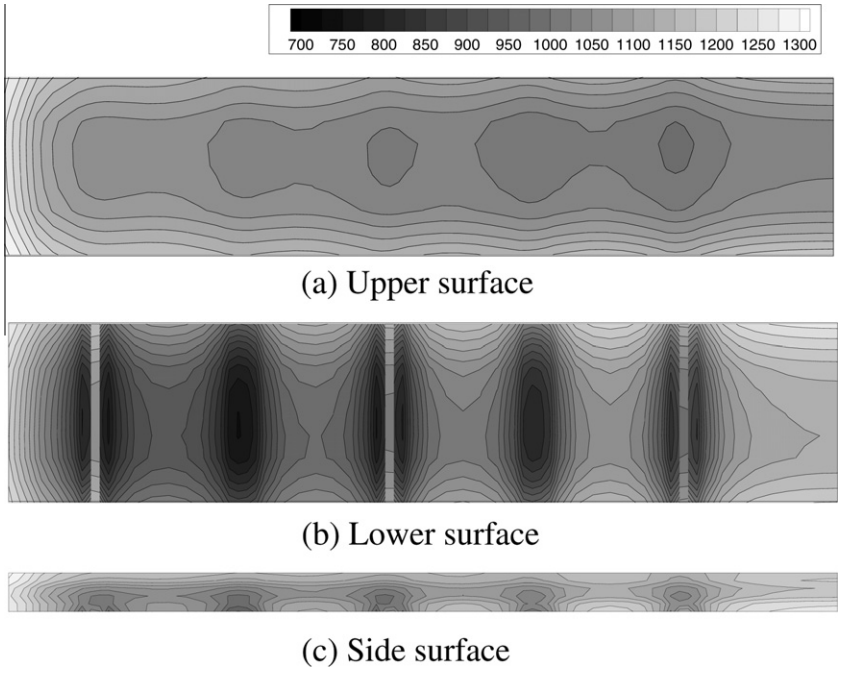

Fig. 6. Temperature contour of the 10th slab just before move.

their head up to the outlet of upper zone, the lower surface is less exposed to the hot gas flows than the upper surface. The lower surface takes about two times longer than the upper surface to complete the growth of radiative heat flux. Radiative heat flux to the upper surface of a slab has a plateau which extends from the 5th slab to the 15th slab. However radiative heat flux to the lower surface of a slab has a single sharp peak at the 12th slab. Radiative heat flux to the upper surface dips at the necks of the furnace roof.

Fig. 8 shows a volume averaged temperature, area averaged temperature on the lower and upper surfaces, and skid mark severity of the slabs inside the furnace before they move. The profiles are also historic curves of a slab from insertion to emission. Skid mark severity is defined here as the difference between the mean temperature on the lower surface and the average temperature at the contact regions. Skid mark severity represents the degree of non-uniform temperature distribution aroused by skid system's shielding heat from hot gas to the slab. A slab enters the heating zone at the temperature of 1058 K and leaves the zone at the temperature of 1352 K. Slabs exit the reheating furnace to rolling mill at about 1503 K.

Slabs experience a relatively large temperature difference between the upper surface and the lower surface until the 11th slab location. This is due to the large difference in the radiative heat fluxes of the two surfaces as depicted in Fig. 8. The temperature difference remains very small after the 12th slab location. The volume average temperature always stays lower than the average temperatures of two surfaces. The upper surface has a higher temperature than the lower surface until the 20th slab location. A reversion occurs in the average temperatures of the two surfaces at the 21st slab location; however, the temperature difference between the two surfaces still remains very small.

A slab has a skid mark severity of 18 K at the first slab location. Skid mark severity continues to grow in the preheating zone and it reaches a maximum value of 162 K at the end of the preheating

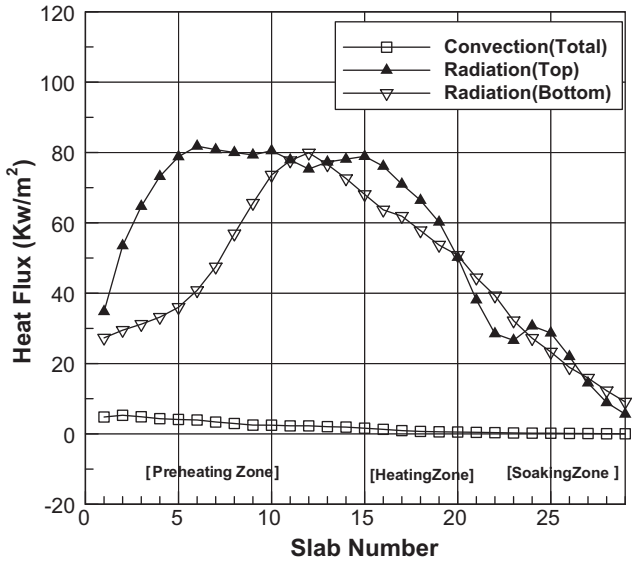

Fig. 7. Various heat fluxes just before move.

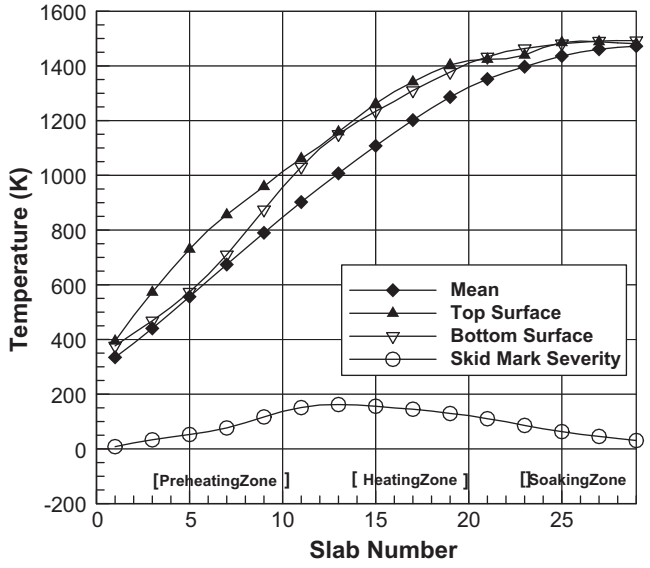

Fig. 8. Temperature profiles just before.

zone. As soon as the slab enters the heating zone, the skid mark severity continues to decrease. The slab enters the soaking zone with the skid mark severity of 100 K. The skid mark severity goes down below 50 K from the 27th slab location in the soaking zone. Finally, the skid mark severity is reduced to 37 K at the time of exit, so that a slab satisfies the requirement of skid mark severity when it is emitted to the rolling mill.

4. Conclusion

An unsteady simulation using the commercial code FLUENT has been performed to investigate the heating characteristics of slabs in a reheating furnace. A user defined program has been written in C language and linked with FLUENT to process the movement of slabs inside the furnace. Unsteady calculation is preformed until it reached a periodically transient solution. Precise observations of slabs heating characteristics are carried out for the given operating conditions.

A slab is mostly heated in the preheating and heating zones. The temperature of the slab is raised very little in the soaking zone, but the degree of temperature uniformity is developed further in the soaking zone. The mean temperature of the slab is increased by 1059 K in the preheating and heating zones, while it is increased by only 151 K in the soaking zone. So, the temperature of the slab is elevated from 293 K to 1503 K in the reheating furnace. Most heat transfer to the slab is done by means of radiation and convective heat transfer contributes little to heating the slab. Over 96% of total heat transfer to the slab is by means of radiation. The time-averaged heat transfer rate to all the slabs inside the furnace is 33,920 kW which corresponds to 46.1% of the total input energy.

When a slab is heated in a reheating furnace, strong temperature gradients are developed at the corners, the edges, and the contact areas of the slab. The temperature gradients around the corners and edges are developed because the slab had a larger thermal resistivity on its corners and edges than on the plane surface. The temperature gradients around the contact regions are due to skid system's heat shielding from hot gas to the slab. As the time goes, the temperature gradients around corners and edges disappear before the slab entered the soaking zone. The temperature gradients around the contact areas of a slab are removed just before the slab was emitted to the rolling mill. When a slab enters the soaking zone, the skid mark severity is 100 K. Skid mark severity goes down below 50 K from the 27th slab location in the soaking zone. Skid mark severity is reduced to 37 K at the time of exit. So a slab satisfies the requirement of skid mark severity when it is emitted to the rolling mill.

Acknowledgement

This work was conducted on behalf of the Korean Ministry of Land, Transport and Maritime Affairs under a program called "Development of Technology for CO_2 Marine Geological Storage".

References

[1] Z. Li, P.V. Barr, J.K. Brimacombe, Computer simulation of the slab reheating furnace, Can. Metall. Quart. 27 (1988) 187–196.
[2] S.H. Han, S.W. Baek, S.H. Kang, C.Y. Kim, Numerical analysis of heating characteristics of a slab in a bench scale reheating furnace, Int. J. Heat Mass Transfer 50 (2007) 2019–2023.
[3] C. Zhang, T. Ishii, S. Sugiyama, Numerical modeling of the thermal performance of regenerative slab reheat furnaces, Numer. Heat Transfer A 32 (1997) 613–631.
[4] J.G. Kim, K.Y. Huh, Three dimensional analysis of the walking beam type reheating furnace in hot strip mills, Numer. Heat Transfer A 38 (2000) 589–609.
[5] J.G. Kim, K.Y. Huh, Prediction of transient slab temperature distribution in the re-heating furnace of a walking-beam type for rolling of steel slabs, ISIJ Int. 40 (2000) 1115–1123.
[6] C.T. Hsieh, M.J. Huang, S.T. Lee, C.H. Wang, Numerical modeling of a walking beam type slab reheating furnace, Numer. Heat Transfer A 53 (2008) 966–981.
[7] M.J. Huang, C.T. Hsieh, S.T. Lee, C.H. Wang, A coupled numerical study of slab temperature and gas temperature in the walking-beam-type slab reheating furnace, Numer. Heat Transfer A 54 (2008) 625–646.
[8] FLUENT 6.3 User's Guide, Fluent Inc., Lebanon, 2006.
[9] FLUENT 6.3 UDF Manual, Fluent Inc., Lebanon, 2006.
[10] R.W. Bilger, Turbulent jet diffusion flames, Prog. Energy Combust. Sci. 1 (1976) 87–109.
[11] P.A. Libby, F.A. Williams, Turbulent Reacting Flows, Academic Press, New York, 1994.
[12] M.F. Modest, Radiative heat transfer, McGraw-Hill Inc., New York, 1993.
[13] B.G. Carlson, K.D. Lathrop, Transport Theory – The Method of Discrete Ordinated in Computing Methods in Reactor Physics, Gordon & Breach Science Publishers, New York, 1968.
[14] J.C. Chai, H.S. Lee, S.V. Patankar, Finite volume method for radiation heat transfer, J. Thermophys. Heat Transfer 8 (1994) 419–425.
[15] S.W. Baek, M.Y. Kim, J.S. Kim, Nonorthogonal finite-volume solutions of radiative heat transfer in a three-dimensional enclosure, Numer. Heat Transfer B 34 (1998) 419–437.
[16] M.F. Modest, The weighted-sum-of-gray-gases model for arbitrary solution methods in radiative transfer, ASME J. Heat Transfer 113 (1991) 650–656.
[17] C.E. Choi, S.W. Baek, Numerical analysis of a spray combustion with nongray radiation using weighted sum of gray gases model, Combust. Sci. Technol. 115 (1996) 297–315.